https://doi.org/10.1016/j.combustflame.2017.04.008

On flame height of circulation-controlled firewhirls with variable physical properties and in power-law vortices: A mass-diffusivity-ratio model correction

Dehai Yu and Peng Zhang*

Department of Mechanical Engineering, the Hong Kong Polytechnic University, Kowloon, Hong Kong

Abstract

This paper presents a theory on the flame height of circulation-controlled firewhirls, approximately combining variable physical properties, a power-law vortex model, and a mass-diffusivity-ratio model. The theoretical results show that the dimensionless flame height can be expressed as a multiplication of four dimensionless factors. The first factor is the stoichiometric-mixture-fraction-scaled Peclet number that was first identified by Chuah *et al*. (*Proc. Combust. Inst.* **33**, 2011) in their theory based on the assumptions of Burgers vortex and constant physical properties. The second factor characterizes the axial flame-stretching effect found by Klimenko and Williams (*Combust. Flame* **160**, 2013) in their theory based on the assumptions of power-law strong vortex and constant physical properties. The third factor quantifies the effect of variable density, which was recently unveiled in Yu and Zhang's theory (*Proc. Combust. Inst.* **36**, 2017). The last factor describes the effect of distinct mass diffusivities of fuel and oxidizer, which has not been considered in the previous studies. Although integrating the first three factors in the theory would lead to an over-prediction to the flame height, accounting for the distinct mass diffusivities of fuel and oxidizer, leading to a mass-diffusivity-ratio model correction, results in the finding of a "reduction" mechanism for the flame height, which is comparable in order of magnitude with the other "enhancement" mechanisms obtained from considering either the power-law strong vortex or variable density.

*Corresponding author
E-mail: pengzhang.zhang@polyu.edu.hk
Fax: (852)23654703 Tel: (852)27666664

Keywords: Firewhirl; Flame height; Variable physical properties; Power-law vortex; Coupling function

Nomenclature

Physical quantities

a	strain rate of vortical flow
c	correction function in matching solutions of coupling function
c_p	constant-pressure specific heat
$d_0(r_0)$	diameter (radius) of the fuel liquid pool
D	mass diffusivity
p	pressure
q_c	heat of combustion per unit mass of fuel
q_v	latent heat of vaporization per unit mass of fuel
r, x, ϕ	cylindrical coordinates
r_c	vortex core radius in physical coordinate
x_h	flame height location
T	temperature
T_f	flame temperature
T_w	ground temperature
T_m	representative temperature
u, v, w	velocity components in x, r, ϕ directions
$\hat{u}, \hat{v}$	velocity components in $\xi - \eta$ coordinate
W	molar weight
X	molar fraction
Y	mass fraction
Z_{st}	stoichiometric mixture fraction
α_v	exponent in power-law vortex model (outside vortex core)
α_v'	exponent in power-law vortex model (inside vortex core)
$\alpha_{v,\mathrm{eff}}$	effective exponent in power-law vortex model

α_T parameter characterizing temperature-dependent mass diffusivity

α_D ratio of fuel mass diffusivity to oxidizer mass diffusivity, $\alpha_D = D_F/D_O$

χ_h flame height location in $\chi - \zeta$ coordinate

δ_{FN} average collision diameter $\delta_{FN} = (\delta_F + \delta_N)/2$

δ_{ON} average collision diameter $\delta_{ON} = (\delta_O + \delta_N)/2$

λ thermal conductivity

ν kinematic viscosity

Ω_{FN} collision integral between fuel and nitrogen molecules

ρ density

σ_{FO} stoichiometric mass ratio $\sigma_{FO} = \nu_O' W_O/(W_F \nu_F')$

η_c the vortex core radius in $\xi - \eta$ space.

Average quantities at $x = 0$

$Q_0 = \frac{1}{r_0}\int_0^{r_0} Q(0,r)dr$, $Q = (T, u, Y_F, \rho, D)$

T_0' modified temperature $T_0' = T_0 - q_v/c_p$

Non-dimensional and normalized variables

A integral factor in far-field solution of coupling functions

Le Lewis number $Le = \lambda/\rho c_p D$

Pe Peclet number $Pe = u_0 d_0/D_{F0}$

$\tilde{Q} = Q/Q_0$, $Q = (D, Y_F, \rho, p)$

$(\tilde{r}, \tilde{x}) = (r, x)/r_0$

$\tilde{T} = c_p T/q_c$

$(\tilde{u}, \tilde{v}) = (u, v)/u_0$

$\tilde{Y}_O = Y_O/\sigma_{FO}$

$\beta_F = \tilde{Y}_F + \tilde{T}$

$\beta_O = \tilde{Y}_O + \tilde{T}$

Transformed coordinates

(χ, ζ) stream function coordinates

(ξ, η) density-mass-diffusivity-weighted coordinates

Subscripts

O	physical quantities of the oxidizer
F	physical quantities of the fuel
N	physical quantities of nitrogen as inert gas
0	physical quantities at $x = 0$
∞	physical quantities in the far field

1. Introduction

As a natural phenomenon that often occurs in wild and urban fires and holds potential to cause severe damages to lives and property, firewhirls have attracted numerous experimental and theoretical studies in the past decades [1-19]. There are particular interests in understanding the controlling mechanism for the flame height of firewhirls because it is a crucial parameter for characterizing a firewhirl [3-5, 9, 10, 19]. For example, the increase of flame height can enhance the radiant energy flux transmitted to the ambience, leading to the spread of spot fires in distance.

The present study is concerned with the circulation-controlled firewhirls experimentally investigated by Chuah *et al.* [5], in which strong firewhirls were observed to preserve their orientation to be perpendicular to the inclined fuel pool surface. This observation implies that these firewhirls were controlled by flow circulation instead of buoyance, which would otherwise turn the firewhirls to the vertical direction. To interpret the experimental observation, Chuah *et al.* proposed a theory for the firewhirls with large Peclet number and derived a dimensionless formula for the flame height as

$$\frac{x_h}{d_0} = \frac{Pe}{16Z_{st}} \tag{1}$$

To derive this equation, Chuah *et al*. assumed that the vortical flow of the firewhirls can be approximated as a Burgers vortex, that the density and physical properties are constants throughout the flow field, and that the Lewis number is unity to invoke a mixture-fraction formulation. Although the theory predicts the right trend that the scaled flame height, x_h/d_0, changes linearly with the stoichiometric-mixture-fraction-scaled Peclet number, $Pe/(16Z_{st})$, it significantly underestimates the flame heights in the presence of strong vortical flows [5].

Klimenko and Williams [9] revisited Chuah *et al.*'s firewhirl theory by using a similar mixture-fraction formulation but replacing the Burgers vortex model by a strong vortex model, because the Burgers vortex was found to be insufficiently strong to describe the realistic vortices, such as tornadoes, hurricanes [20] and firewhirls [9]. A revised formula for flame height, retaining the linear relation of Equation (1), contains an additional multiplicative factor, $2/\alpha_v$, as follows

$$\frac{x_h}{d_0} = \frac{2}{\alpha_v}\frac{Pe}{16Z_{st}} \tag{2}$$

This factor originates from the power-law model of strong vortices, in which the stream function is given by

$$\psi(r,x) = s(x)r^{\alpha_v} \tag{3}$$

and the velocity components are

$$u(r,x) = \frac{1}{r}\frac{\partial\psi}{\partial r} = \alpha_v s(x)r^{\alpha_v-2}, \qquad v(r,x) = -\frac{1}{r}\frac{\partial\psi}{\partial x} = -s'(x)r^{\alpha_v-1} \tag{4}$$

Here $s'(x)$ denotes the first-order derivative of $s(x)$. By setting $\alpha_v = 2$, Equation (2) can degenerate to Equation (1) because Equations (3) and (4) degenerate to the stream function and velocity components of the Burgers vortex, respectively. However, the exponent α_v must fall below 2 in realistic strong vortices.

Figure 1 shows the radial profiles of the scaled axial velocity, $u(x,r)/s(x)$, and the scaled radial velocity, $-v(x,r)/s'(x)$. It is seen that the magnitudes of the axial and radial velocities of strong vortices (i.e. those with $\alpha_v < 2$) are enhanced significantly in the vicinity of axis, compared with those of Burgers vortex. Moreover, the enhancement of strong vortex increases with decreasing α_v, which varies between 4/3 and 3/2 according to Klimenko's studies [9, 20]. Consequently, Equation (2), with either $\alpha_v = 4/3$ or recommended $\alpha_v = 1.43$, predicts considerable enhancement of flame heights of firewhirls, agreeing well with Chuah *et al.*'s experimental data.

It should be noted that Equation (2) with $\alpha_v < 2$ results in physically unrealistic axial velocity at the axis (i.e. $r = 0$), where the flame height is determined. To remedy the model deficiency, an alternative approach for deriving the flame height was proposed by Klimenko and Williams [9]. To facilitate a self-similar solution, which does not satisfy the boundary condition at the liquid fuel pool but is valid in the far field of the fuel pool, the stream function and velocity components were assumed, being in accordance with the strong vortex approximation, as

$$\psi(r,x) = xf(r), \qquad u = x\frac{f'(r)}{r}, \qquad v = -\frac{f(r)}{r} \tag{5}$$

where the piecewise smooth function $f(r)$ is given by

$$f(r) = \begin{cases} r_c^{\alpha_v - 2} r^2, & r \le r_c \\ r^{\alpha_v}, & r \ge r_c \end{cases} \tag{6}$$

The singularity of the axial velocity at the axis is absent in the modified power-law vortex model by taking into account of a viscous vortex core of radius r_c. The flow in the vortex core is similar to that of the Burgers vortex with $\alpha_v = 2$. Consequently, the influence of the unspecified vortex core radius on the flame height was accounted for in Equation (2) by treating α_v as a fitting parameter, denoted by α_{eff} in the paper of Klimenko and Williams.

In their recent theory of firewhirls [19], Yu and Zhang abandoned the assumption of constant density, which has been proved physically unrealistic in many flame problems. To facilitate the comparison with the previous theories, the assumptions of large Peclet number and unity Lewis number were retained and the Burgers vortex model was still adopted to describe the vortical flow. By analytically solving the problem in the coupling function formulation, Yu and Zhang obtained a flame height formula given by

$$\frac{x_h}{d_0} = \left(\frac{T_m}{T_0}\right)^{2-\alpha_T} \frac{Pe}{16 Z_{st}} \tag{7}$$

The multiplicative factor, $(T_m/T_0)^{2-\alpha_T}$, is always larger than unity and therefore provides another enhancement mechanism for the flame height due to variable density. This is because the "mean" temperature T_m, which denotes an exact albeit complicated integral of flow temperature, is always higher than T_0, and the parameter α_T, which is the exponent in the power-law formula characterizing the temperature-dependence of mass diffusivity, is always less than 2. For $\alpha_T = 1.5$ from the kinetic theory of gases employing rigid-sphere model, and $\alpha_T = 1.8$ suggested by Chuah *et al.* [5], the predictions of Equation (7) agree well with Chuah *et al.*'s experimental data.

It is seen that Equations (2) and (7) provide distinctly different "enhancement" mechanisms for predicting the flame heights, both reveal essential physics of the circulation-controlled firewhirls, and separately lead to results agreeing well with the experimental observations. The present study was motivated by integrating these two independent mechanisms into a unified formulation. It was subsequently found that any simple combination of these mechanisms could overshoot the experimental data of flame heights, implying that additional "loss" mechanisms may have been overlooked in the previous studies. Inspired by the classical results on single droplet combustion in a quiescent environment [21], that the d^2-law theory based on the unity-Lewis-number and equal-diffusivity assumptions significantly overestimates the flame standoff distance, and accounting for that the much smaller diffusivity of fuel vapor compared with that of oxidizer can substantially reduce the distance, we hypothesized that the dissimilar diffusivities of liquid fuel and air in Chuah *et al.*'s experiments might play a similar role of reducing the flame height. Specifically, the shape of the non-premixed firewhirl flame is determined by the local stoichiometry; the smaller mass-diffusivity of fuel vapor results in that the iso-surface of stoichiometry tends to move towards the fuel pool.

Based on the above considerations, we established a theory to investigate the flame heights of circulation-controlled firewhirls by integrating the following three factors. First, the physical properties such as density and mass diffusivity are treated as variables. Second, the mass diffusivities are distinct on the fuel and oxidizer sides of the flame. Third, a singularity-free power-law vortex model, consisting two power-law regimes with different exponents, is adopted. In section 2, a steady, axisymmetric firewhirl system is mathematically formulated and analytically solved in terms of coupling functions by invoking the unity-Lewis-number approximation. In section 3, a flame height expression is presented and the contributing components are discussed in detail for their physical meanings.

2. Mathematical Formulation

2.1 Coupling-function Formulation

A circulation-controlled firewhirl is modelled as a steady non-premixed flame in a forced axisymmetric vortical flow without buoyance effects [5, 9]. By following the previous studies [5, 9, 19], we assume that the Lewis number is unity throughout the flow field to invoke a coupling-function formulation. However, we abandoned the assumption of constant physical properties by considering not only variable density but also distinct, variable transport properties on the fuel and oxidizer sides of the flame, and as such we have

$$Le_F = \frac{\lambda_F}{\rho c_p D_F} = 1;\ Le_O = \frac{\lambda_O}{\rho c_p D_O} = 1;\ \lambda_F \neq \lambda_O;\ D_F \neq D_O \tag{8}$$

Consequently, the present problem can be characterized by two species-enthalpy coupling functions, namely, β_F and β_O. It is noted that the species coupling functions adopted in the authors' previous paper are not applicable because of the distinct mass diffusivities for fuel and oxidizer. The transport equations for β_F and β_O are given by

$$\rho u \frac{\partial \beta_F}{\partial x} + \rho v \frac{\partial \beta_F}{\partial r} - \frac{\partial}{\partial x}\left(\rho D_F \frac{\partial \beta_F}{\partial x}\right) - \frac{1}{r}\frac{\partial}{\partial r}\left(\rho D_F r \frac{\partial \beta_F}{\partial r}\right) = 0 \tag{9a}$$

$$\rho u \frac{\partial \beta_O}{\partial x} + \rho v \frac{\partial \beta_O}{\partial r} - \frac{\partial}{\partial x}\left(\frac{1}{\alpha_D}\rho D_F \frac{\partial \beta_O}{\partial x}\right) - \frac{1}{r}\frac{\partial}{\partial r}\left(\frac{1}{\alpha_D}\rho D_F r \frac{\partial \beta_O}{\partial r}\right) = 0 \tag{9b}$$

The temperature- and pressure-dependent mass diffusivity for binary diffusion (as nitrogen is abundant in the gas mixtures) can be evaluated by using the Chapman-Enskog theory [22]. The ratio of the mass diffusivities is thus given by $\alpha_D = \frac{D_F}{D_O} = \frac{\delta_{FN}^2 \Omega_{FN}\sqrt{1/W_F + 1/W_N}}{\delta_{ON}^2 \Omega_{ON}\sqrt{1/W_O + 1/W_N}}$. Because the temperature- and pressure-dependent factors of D_F and D_O have been cancelled out in deriving the equation, α_D can be regarded as a constant in the entire flow field, only dependent on the fuel type.

Equations (9a) and (9b) are rigorously valid on the fuel and oxidizer sides of the flame sheet, respectively, and are approximate on the other side. The exact solutions must be determined by matching β_F and β_O at the flame sheet, where both reactants vanish and temperature is the flame temperature T_f, rendering $\beta_F = \beta_O = T_f$ [21]. Although such a matching solution approach works

for one-dimensional flames such as the classical droplet flame, it is however mathematically inapplicable to the present problem because the general solution to the partial differential equations (9a) and (9b) cannot be obtained without the prescribed boundary conditions at the two-dimensional flame sheet. In order to resolve the mathematical difficulty, we proposed an approximate matching solution procedure, which will be applied to the parabolized version of Equations (9a) and (9b) in Section 3.3.

The corresponding boundary conditions (denoted by BC for short and hereinafter) are given by

BC(1), at $r = 0$

$$\frac{\partial \beta_F}{\partial r} = \frac{\partial \beta_O}{\partial r} = 0$$

BC(2), at $r \to \infty$

$$\frac{\partial \beta_F}{\partial r} = \frac{\partial \beta_O}{\partial r} = 0$$

BC(3a), at $x = 0$ and $r \le r_0$

$$\rho u \beta_F - \rho D_F \frac{\partial \beta_F}{\partial x} = \rho u \left(1 + \tilde{T}_0 - \frac{q_v}{q_c}\right)$$

$$\rho u \beta_O - \frac{1}{\alpha_D} \rho D_F \frac{\partial \beta_O}{\partial x} = \rho u \left(\tilde{T}_0 - \frac{q_v}{q_c}\right)$$

BC(3b), at $x = 0$ and $r > r_0$

$$\frac{\partial \beta_F}{\partial x} = \frac{\partial \beta_O}{\partial x} = 0$$

BC(4), at $x \to \infty$

$$\beta_F = \tilde{T}_\infty, \qquad \beta_O = \tilde{Y}_{O\infty} + \tilde{T}_\infty$$

BC(1) and BC(2) refer to the boundary conditions at the axis and in the far field, respectively. BC(3a) describes the Stefan flow in the evaporation layer, where the diffusive and convective transport of fuel along the axial direction is balanced by the fuel evaporation, and the energy required by the evaporation is supplied by the heat transported from the flame. The absence of radial derivatives can be attributed to that the radial dimension of the evaporation layer is significantly larger than the axial dimension. Consequently, the convective and diffusive transport in the axial direction dominate over those in the radial direction. Mathematically, integrating the transport equations for energy and

species in the axial direction, neglecting the radial convection and diffusion terms, we can obtain BC(3a). The derivation of BC(3a) can be briefly described in the following. The axial flux of convection and diffusion of oxidizer is zero, i.e. $\rho u Y_O - \rho D_O \partial Y_O/\partial x = 0$ because oxidizer is not condensable. The total flow flux, ρu, is attributed only to the combined convective and diffusive fluxes of fuel, i.e. $\rho u Y_F - \rho D_F \partial Y_F/\partial x = \rho u$. As far the enthalpy transport, the net enthalpy flux, $\rho u c_p (T - T_0)$, is equal to the heat conduction flux, $\lambda \partial T/\partial x$, subtracted by the amount required by vaporization, $\rho u q_v$. Similar but more general conservation conditions at an interface can be found in [23]. BC(3b) describes the non-vaporizing surface outside fuel pool. BC(4) indicates that there is no fuel on the oxidizer side of the flame, a result from the flame sheet assumption [21, 24].

2.2 Coordinate Transformation

Following the same approach adopted in the previous study [19], we introduced a density-mass-diffusivity-weighted coordinate system in the form of

$$\xi = \frac{D_{F0}}{u_0 r_0}\int_0^{\tilde{x}} \tilde{\rho}^2 \widetilde{D}_F dx' = \frac{2}{Pe}\int_0^{\tilde{x}} \tilde{\rho}^2 \widetilde{D}_F dx', \qquad \eta = \int_0^{\tilde{r}} \tilde{\rho} dr' \tag{10}$$

The transformation (10) is analogous to the well-known Howarth-Dorodnitsyn transformation [25, 26], which is widely used in self-similar compressible boundary layer problems. It should be noted that the present problem is not a self-similar flow because of the characteristic length scale r_0. A valuable self-similar solution can however be derived at the far field of fuel pool [9] and will be discussed shortly in the following section.

Applying the coordinate transformation to Equations (9a) and (9b) as well as the boundary conditions BC(1)-(4), yields

$$\hat{u}\frac{\partial \beta_F}{\partial \xi} + \hat{v}\frac{\partial \beta_F}{\partial \eta} = \frac{4}{Pe^2 \tilde{\rho}}\left(\frac{\partial}{\partial \xi} + h\frac{\partial}{\partial \eta}\right)\left[\tilde{\rho}^3 \widetilde{D}_F^2 \left(\frac{\partial \beta_F}{\partial \xi} + h\frac{\partial \beta_F}{\partial \eta}\right)\right] + \left(\frac{2g}{Pe\tilde{\rho}\tilde{r}}\frac{\partial}{\partial \xi} + \frac{1}{\tilde{\rho}^2 \widetilde{D}_F \tilde{r}}\frac{\partial}{\partial \eta}\right)\left(\frac{2\tilde{\rho}^3 \widetilde{D}_F^2 g\tilde{r}}{Pe}\frac{\partial \beta_F}{\partial \xi} + \tilde{\rho}^2 \widetilde{D}_F \tilde{r}\frac{\partial \beta_F}{\partial \eta}\right) \tag{11}$$

$$\hat{u}\frac{\partial \beta_O}{\partial \xi}+\hat{v}\frac{\partial \beta_O}{\partial \eta}$$
$$=\frac{4}{\alpha_D Pe^2\tilde{\rho}}\left(\frac{\partial}{\partial \xi}+h\frac{\partial}{\partial \eta}\right)\left[\tilde{\rho}^3\widetilde{D}_F^2\left(\frac{\partial \beta_O}{\partial \xi}+h\frac{\partial \beta_O}{\partial \eta}\right)\right]$$
$$+\frac{1}{\alpha_D}\left[\frac{2g}{Pe\tilde{\rho}\tilde{r}}\frac{\partial}{\partial \xi}+\frac{1}{\tilde{\rho}^2\widetilde{D}_F\tilde{r}}\frac{\partial}{\partial \eta}\right]\left(\frac{2\tilde{\rho}^3\widetilde{D}_F^2 g\tilde{r}}{Pe}\frac{\partial \beta_O}{\partial \xi}+\tilde{\rho}^2\widetilde{D}_F\tilde{r}\frac{\partial \beta_O}{\partial \eta}\right) \tag{12}$$

where we have

$$g(\tilde{x},\tilde{r})=\frac{1}{\tilde{\rho}^2\widetilde{D}_F}\int_0^{\tilde{x}}\frac{\partial}{\partial \tilde{r}}\left(\tilde{\rho}^2\widetilde{D}_F\right)dx',\qquad h(\tilde{x},\tilde{r})=\frac{Pe}{2\tilde{\rho}^2\widetilde{D}_F}\int_0^{\tilde{r}}\frac{\partial \tilde{\rho}}{\partial \tilde{x}}dr' \tag{13}$$

to account for the variations of density and mass diffusivity gradients in axial and radial directions. In addition, the non-dimensional velocity components in Equations (11) and (12) are given by

$$\hat{u}=2\tilde{u}+2g\tilde{v},\qquad \hat{v}=2h\tilde{u}+\frac{Pe}{\tilde{\rho}\widetilde{D}_F}\tilde{v} \tag{14}$$

The detailed derivations in the coordinate transformation have been presented in the Appendix A.

Correspondingly, the boundary conditions BCs (1)-(4) can be rewritten by

BC(1') at $\eta=0$

$$\frac{\partial \beta_F}{\partial \eta}=\frac{\partial \beta_O}{\partial \eta}=0$$

BC(2') at $\eta\to\infty$

$$\frac{\partial \beta_F}{\partial \eta}=\frac{\partial \beta_O}{\partial \eta}=0$$

BC(3a') at $\xi=0$ and $\eta\le 1$

$$\beta_F=1+\tilde{T}_0-\frac{q_v}{q_c}+\frac{4}{Pe^2}\left(\frac{\partial \beta_F}{\partial \xi}\right)+\frac{2\tilde{\rho}^2\widetilde{D}_F h}{Pe}\left(\frac{\partial \beta_F}{\partial \eta}\right)$$

$$\beta_O=\tilde{T}_0-\frac{q_v}{q_c}+\frac{4}{\alpha_D Pe^2}\left(\frac{\partial \beta_O}{\partial \xi}\right)+\frac{2\tilde{\rho}^2\widetilde{D}_F h}{\alpha_D Pe}\left(\frac{\partial \beta_O}{\partial \xi}\right)$$

BC(3b') at $\xi=0$ and $\eta>1$

$$\frac{\partial \beta_F}{\partial \xi} = \frac{\partial \beta_O}{\partial \xi} = 0$$

BC(4') at $\eta \to \infty$

$$\beta_F = \tilde{T}_\infty, \qquad \beta_O = \tilde{Y}_{O\infty} + \tilde{T}_\infty$$

As far as the circulation-controlled firewhirls being concerned, we can apply the large Peclet number approximation, i.e., $Pe \gg 1$, to simply the above equations. Physically, the firewhirl with large Peclet numbers is substantially elongated along the axial direction due to the strong axial convection dominant over the diffusion and the flame height is thus significantly larger than the radius of the fuel pool. Consequently, the axial coordinate is scaled by a factor of $2/Pe$ by the transformation (10) so that the nondimensional velocities $\hat{u}$ and $\hat{v}$ in the $\xi - \eta$ space have the same order of magnitude. As a consequence, we can deduce from Equation (13) that $h \sim O(1), g \sim O(1)$ and $\tilde{u} \sim O(1), \tilde{v} \sim O(Pe^{-1})$, which implies that the radial velocity v in physical coordinate is smaller than u_0 by a factor $1/Pe$.

An alternative way to make the above estimations of orders of magnitude is as follows. We have used the radius of the fuel pool to nondimensionalize the coordinates, so the derivative with respect to the axial coordinate yields an $1/Pe$, which cancels out with a factor of Pe outside the integral in Equation (13), resulting in $h \sim O(1)$. Because $\tilde{\rho}^2 \widetilde{D}_F$ weakly depends on temperature so that its radial derivative is of $O(1/Pe)$, which is cancelled out by another factor of Pe produced from the axial integration of the radial derivative, rendering g to be of $O(1)$.

Based on the above considerations, we can neglect all the terms of $O(Pe^{-1})$ and $O(Pe^{-2})$ in Equations (11) and (12) and then have

$$\hat{u}\frac{\partial \beta_F}{\partial \xi} + \hat{v}\frac{\partial \beta_F}{\partial \eta} = \frac{1}{\eta}\frac{\partial}{\partial \eta}\left(\eta \frac{\partial \beta_F}{\partial \eta}\right) \tag{15a}$$

$$\hat{u}\frac{\partial \beta_O}{\partial \xi} + \hat{v}\frac{\partial \beta_O}{\partial \eta} = \frac{1}{\alpha_D}\frac{1}{\eta}\frac{\partial}{\partial \eta}\left(\eta \frac{\partial \beta_O}{\partial \eta}\right) \tag{15b}$$

To derive Equations (15a) and (15b), we have invoked an approximation that

$$\frac{\tilde{\rho}^2 \widetilde{D}_F \tilde{r}}{\int_0^{\tilde{r}} \tilde{\rho} dr'} = C(\xi)$$

(16)

is independent of the coordinate η. This approximation is a weaker version of the widely-used Chapman-Rubesin approximation, which further assumes $C(\xi)$ be a global constant [27]. Accordingly, the boundary conditions BCs (1')-(4') become

BC(i) at $\eta = 0$,

$$\frac{\partial \beta_F}{\partial \eta} = \frac{\partial \beta_O}{\partial \eta} = 0$$

BC(ii) at $\eta \to \infty$,

$$\frac{\partial \beta_F}{\partial \eta} = \frac{\partial \beta_O}{\partial \eta} = 0$$

BC(iiia) at $\xi = 0$ and $\eta \leq 1$,

$$\beta_F = \tilde{Y}_{F0} + \tilde{T}_0', \qquad \beta_O = \tilde{T}_0'$$

BC(iiib) at $\xi = 0$ and $\eta > 1$,

$$\beta_F = \tilde{T}_\infty, \qquad \beta_O = \tilde{T}_\infty + \tilde{Y}_{O\infty}$$

The mixed boundary condition BC(3a') is replaced by the Dirichlet boundary condition BC(iiia) for mathematical convenience without losing the physics because the determination of the fuel vapor concentration Y_{F0} requires BC(3a'). The coupling function is valid in the whole flow field so that β_F and β_O must satisfy BC(iiia), given the quantities on the evaporating fuel pool are known. BC(iiib) actually implies an isothermal ground surface outside the pool flame. Such a boundary condition is not required by the previously theories [5, 9] based on the mixture fraction formulation, but it brings significant mathematical convenience to the theoretical analysis based on the coupling function formulation, resulting in the Burke-Schumann-like solutions produced by the mixture fraction formulations [5, 9]. One could formulate a theory with a prescribed ground temperature profile $\tilde{T}_w$, which however lacks experimental data and causes unnecessary mathematical complexities. Furthermore, the wall temperature $\tilde{T}_w$, being scaled by the heat of combustion q_c/c_p, is much smaller than the flame temperature $\tilde{T}_f$ and the mass fractions $\tilde{Y}_F$ and $\tilde{Y}_O$. In consequence, replacing $\tilde{T}_\infty$ by $\tilde{T}_w$ in the solutions of β_F and β_O is unlikely to make significant difference. Moreover, BC(4) is not needed for solving Equations (15a) and (15b) which are parabolic partial differential equations.

Because the fuel pool is in condensed phase, the physics of Stefan flow at the evaporating surface should be considered to derive three auxiliary equations to determine the fuel vapor mass fraction Y_{F0}, the Stefan flow velocity u_0, and the temperature T_0, for closuring the two-phase problem. The details of the derivations have been given in [19] and will be briefly described here. First, the axial diffusive and convective transport of fuel feeding the flame is balanced by the fuel evaporation from liquid phase to gaseous phase, yielding a mass balance equation. Second, the energy required by the evaporation is supplied by the heat transport from the flame, yielding the energy balance equation. Third, the Clausius-Clapeyron equation is needed to relate Y_{F0} and T_0. In addition, the equation of state and the Bernoulli's equation can be used to determine the pressure p_0 and the density ρ_0 on the evaporation layer. For the present focus of establishing a relation between the diameter-scaled flame height x_h/d_0 and modified Peclet number $Pe/(16Z_{st})$, we can assume those physical quantities on the evaporation are prescribed. It should be also noted that only axial transport is considered to derive the auxiliary equations for the problem closure because of the large Peclet number assumption. Therefore the equations cannot be applied in the $O(1/Pe)$ neighborhood of the origin, where the assumption is invalid.

2.3 Power-law Vortex Model

In Chuah *et al.*'s theory, the vortical flow was assumed to be a Burgers vortex, whose stream function contains a second-order power function of the radial coordinate, namely, Equation (3) with $\alpha_v = 2$ [5]. To characterize the strong vortical flow of firewhirls, Klimenko and Williams adopted a power-law vortex model expressed in Equation (3) with $1 < \alpha_v < 2$ and further introduced a Burgers vortex core to eliminate the velocity singularity at the axis. To generalize these models, we assume that the stream function of the vortical flow can be described by a piecewise power-law vortex model in the $\xi - \eta$ space as

$$\psi = \begin{cases} s(\xi)\eta^{\alpha_v'}, & \eta < \eta_c \\ \eta_c^{\alpha_v'-\alpha_v} s(\xi)\eta^{\alpha_v}, & \eta \geq \eta_c \end{cases} \tag{17a}$$

and the resulting velocity components are given by

$$\hat{u} = \begin{cases} \alpha_v' \eta^{\alpha_v'-2} s(\xi), & \eta < \eta_c \\ \alpha_v \eta_c^{\alpha_v'-\alpha_v} s(\xi) \eta^{\alpha_v-2}, & \eta \geq \eta_c \end{cases}, \qquad \hat{v} = \begin{cases} -s'(\xi) \eta^{\alpha_v'-1}, & \eta < \eta_c \\ -\eta_c^{\alpha_v'-\alpha_v} s'(\xi) \eta^{\alpha_v-1}, & \eta \geq \eta_c \end{cases}$$

(17b)

where η_c is the radius of the vortex core and $s(\xi)$ is subject to other conservation laws and boundary conditions. α_v', the exponent of the power law model in the inner regime, must be larger than or equal to 2 to avoid the velocity singularity at the axis, which does not physically exist in firewhirls. Furthermore, we can make use of $\eta_c \ll 1$, which physically means that the radius of the vortex core is sufficiently smaller than that of the fuel pool.

A few remarks should be given to the present vortex model. By transforming $\hat{u}$ and $\hat{v}$ back to the physical coordinates, we can have the velocity field satisfying the continuity equation, indicating that the power-law vortex in the $\xi - \eta$ space is physically realistic. The detailed derivations are presented in Appendix B. In the vortex models of the present study and Klimenko and Williams [9], a discontinuity of the axial velocity exists at the edge of the vortex core. The discontinuity can however be readily eliminated by adding higher order correction term of $O\left(\eta^{\alpha_v'+1}\right)$ to the inner part of the stream function. Because the term decreases at least cubically (as $\alpha_v' \geq 2$) with the radius of vortex core, neglecting the discontinuity does not cause any significant influence on the flame height. Furthermore, it is noted that the exponents in the stream function may slightly change with density variation. Nevertheless, the circulation-controlled firewhirls addressed in the present study presumes that the vortical flow field is so strong that it is unlikely to be substantially affected by the density variation, and that the functional form of the vortex model should remain as the power-law functional forms suggested by Klimenko and Williams [9].

2.4 Stream Function Coordinates

In order to facilitate analytical solutions of Equations (15a) and (15b) subject to the boundary conditions of BC(i), BC(ii) and BC(iii), we introduce the stream function coordinates, defined by

$$\chi = \frac{\alpha_v}{2} \xi, \qquad \zeta = \sqrt{2\psi}$$

(18)

Similar transformation in the dimensional form were adopted by Klimenko and Williams [9]. Applying Equation (18) to Equations (15a) and (15b), we have

$$\frac{\partial \beta_F}{\partial \chi} = \frac{1}{\zeta}\frac{\partial}{\partial \zeta}\left(\zeta \frac{\partial \beta_F}{\partial \zeta}\right) \tag{19a}$$

$$\frac{\partial \beta_O}{\partial \chi} = \frac{1}{\alpha_D}\frac{1}{\zeta}\frac{\partial}{\partial \zeta}\left(\zeta \frac{\partial \beta_O}{\partial \zeta}\right) \tag{19b}$$

Accordingly, the boundary conditions in the stream function coordinates are given by

BC(I) at $\zeta = 0$

$$\frac{\partial \beta_F}{\partial \zeta} = \frac{\partial \beta_O}{\partial \zeta} = 0$$

BC(II) at $\zeta \to \infty$

$$\frac{\partial \beta_F}{\partial \zeta} = \frac{\partial \beta_O}{\partial \zeta} = 0$$

BC(III-a) at $\chi = 0$ and $\zeta \leq 1$

$$\beta_F = \tilde{Y}_{F0} + \tilde{T}_0', \qquad \beta_O = \tilde{T}_0'$$

BC(III-b) at $\chi = 0$ and $\zeta > 1$

$$\beta_F = \tilde{T}_\infty, \qquad \beta_O = \tilde{T}_\infty + \tilde{Y}_{O\infty}$$

Equation (19a) and (19b) together with BCs (I)-(III) formulate an analytically solvable PDE system describing the firewhirls.

3. Flame Height of Firewhirls

3.1 Approximate Matching Solutions of Coupling Functions

Similar to Equations (9a) and (9b), Equations (19a) and (19b) are rigorously valid on the fuel and oxidizer sides of the flame sheet, and are approximate on the other side. The exact solution must be obtained by means of matching at the flame sheet location, as we have discussed in the preceding section. Considering that the rigorous matching of the solutions of Equations (19a) and (19b) is

analytically impossible, recognizing that the two equations are linear and almost identical (except the factor $1/\alpha_D$), and noting that the far-field and axisymmetric boundary conditions are formally valid for β_F and β_O, we constructed the approximate matching solutions in the form of

$$\beta_F(\chi,\zeta) = \beta_F^{(0)}(\chi,\zeta) + c_F(\chi,\zeta)\beta_F^{(1)}(\chi,\zeta) \tag{20}$$

$$\beta_O(\chi,\zeta) = \beta_O^{(0)}(\chi,\zeta) - c_O(\chi,\zeta)\beta_O^{(1)}(\chi,\zeta) \tag{21}$$

where

$$\beta_F^{(0)} = \tilde{T}_\infty + \left(\tilde{Y}_{F0} + \tilde{T}_0' - \tilde{T}_\infty\right)\int_0^\infty J_0(\omega\zeta)J_1(\omega)\exp(-\omega^2\chi)\,d\omega$$

$$\beta_O^{(0)} = \tilde{T}_\infty + \tilde{Y}_{O\infty} + \left(\tilde{T}_0' - \tilde{T}_\infty - \tilde{Y}_{O\infty}\right)\int_0^\infty J_0(\omega\zeta)J_1(\omega)\exp\left(-\frac{\omega^2}{\alpha_D}\chi\right)d\omega$$

are the leading order solutions obtained by formally extending Equations (19a) and (19b) to the entire flow field, and

$$\beta_F^{(1)} = \left(\tilde{Y}_{F0} + \tilde{T}_0' - \tilde{T}_\infty\right)\int_0^\infty J_0(\omega\zeta)J_1(\omega)\left[\exp\left(-\frac{\omega^2}{\alpha_D}\chi\right) - \exp(-\omega^2\chi)\right]d\omega$$

$$\beta_O^{(1)} = \left(\tilde{T}_0' - \tilde{T}_\infty - \tilde{Y}_{O\infty}\right)\int_0^\infty J_0(\omega\zeta)J_1(\omega)\left[\exp\left(-\frac{\omega^2}{\alpha_D}\chi\right) - \exp(-\omega^2\chi)\right]d\omega$$

are the first-order corrections due to the factor $1/\alpha_D$. $c_F(\chi,\zeta)$ and $c_O(\chi,\zeta)$ are bounded functions asymptotically satisfying $c_F(\chi < \chi_h, 0) = c_O(\chi,\infty) = 0$ and $c_F(\chi,\infty) = c_O(\chi < \chi_h, 0) = 1$, which are proved in the Appendix C.

3.2 Far-field Solutions

In the present power-law vortex model, the ξ-dependence of the stream function is described by $s(\xi)$ according to Equation (17a). If the function $s(\xi)$ is assumed to be a linear function of ξ, special far-field solutions of β_F and β_O can be found regardless of the functional form of the

η-dependence of the stream function, which is not restricted to power functions. Such special far-field solutions can be given by

$$\beta_F = \frac{\tilde{Y}_{F0} + \tilde{T}_0' - \tilde{T}_\infty}{2\xi A} \exp\left(\int_0^\eta \hat{v} d\eta'\right) + \tilde{T}_\infty \tag{22}$$

$$\beta_O = \alpha_D \frac{\tilde{T}_0' - \tilde{T}_\infty - \tilde{Y}_{O\infty}}{2\xi A} \exp\left(\alpha_D \int_0^\eta \hat{v} d\eta'\right) + \tilde{T}_\infty + \tilde{Y}_{O\infty} \tag{23}$$

where the constant A is defined by

$$A = \frac{1}{\xi} \int_0^\infty \hat{u} \exp\left(\int_0^\eta \hat{v} d\eta\right) \eta d\eta \tag{24}$$

The solutions (22) and (23) exactly satisfy the governing equations (19a) and (19b), respectively, subject to the boundary conditions BC (I) and BC(II), but they do not satisfy the boundary conditions BC(IIIa) and BC(IIIb). This can be regarded as a variant and generalized version of the result obtained by Klimenko and Williams[9], where a far-field solution of mixture fraction in physical coordinates was obtained for constant physical properties. In Equations (22) and (23), the effects of variable physical properties have been implicitly included in the coordinates η and ξ.

3.3 Flame Height Equation

The flame height can be determined by equating β_F and β_O from Equations (20) and (21), setting ζ_f equal to zero, resulting in the implicit expression for χ_h as $\beta_F(\chi_h, 0) = \beta_O(\chi_h, 0)$, which is written in detailed form by

$$\left(\tilde{Y}_{F0}+\tilde{T}_0'-\tilde{T}_\infty\right)\int_0^\infty J_1(\omega)\exp(-\omega^2\chi_h)\,d\omega$$
$$+c_F(\chi_h,0)\left(\tilde{Y}_{F0}+\tilde{T}_0'-\tilde{T}_\infty\right)\int_0^\infty J_1(\omega)\left[\exp\left(-\frac{\omega^2}{\alpha_D}\chi_h\right)-\exp(-\omega^2\chi_h)\right]d\omega$$
$$=\tilde{Y}_{O\infty}+\left(\tilde{T}_0'-\tilde{T}_\infty-\tilde{Y}_{O\infty}\right)\int_0^\infty J_1(\omega)\exp\left(-\frac{\omega^2}{\alpha_D}\chi_h\right)d\omega$$
$$-c_O(\chi_h,0)\left(\tilde{T}_0'-\tilde{T}_\infty-\tilde{Y}_{O\infty}\right)\int_0^\infty J_1(\omega)\left[\exp\left(-\frac{\omega^2}{\alpha_D}\chi_h\right)-\exp(-\omega^2\chi_h)\right]d\omega \tag{25}$$

where χ_h refers to the flame height location in $\chi-\zeta$ coordiantes.

Evaluating the integrals exactly, we have

$$\int_0^\infty J_1(\omega)\exp(-\omega^2\chi_h)d\omega=1-\exp\left(-\frac{1}{4\chi_h}\right) \tag{26a}$$

$$\int_0^\infty J_1(\omega)\exp\left(-\frac{\omega^2}{\alpha_D}\chi_h\right)d\omega=1-\exp\left(-\frac{\alpha_D}{4\chi_h}\right) \tag{26b}$$

Substituting (26a) and (26b) into (25) and recalling the result that $4\chi_h\gg1$ [5, 9, 19], we can expand the above exponential terms in Taylor series, retain the first order correction, and have

$$\exp\left(-\frac{1}{4\chi_h}\right)\sim1-\frac{1}{4\chi_h},\qquad\exp\left(-\frac{\alpha_D}{4\chi_h}\right)\sim1-\frac{\alpha_D}{4\chi_h} \tag{27}$$

Substituting Equation (27) into Equation (25), we have the flame height expression in the explicit form of

$$\chi_h=\frac{\alpha_D}{4Z_{st}}\left\{1+\frac{Z_{st}(1-\alpha_D)}{\alpha_D}\left[\frac{(1-c_F-c_O)\left(\tilde{T}_0'-\tilde{T}_\infty\right)}{\tilde{Y}_{O\infty}}-(1-c_F)\frac{\tilde{Y}_{F0}}{\tilde{Y}_{O\infty}}+c_O\right]\right\} \tag{28}$$

To further simplify Equation (28), we can make the following estimation of the order of magnitude for the second term in the bracket. The stoichiometric mixture fraction, Z_{st}, is much smaller than

unity for commonly used hydrocarbon fuels [5, 24]. The mass diffusivity ratio α_D is a quantity of order $O(1)$ for the concerned fuels, implying that $(1-\alpha_D)/\alpha_D$ is of order $O(1)$ as well. Moreover, the factor $\left(\tilde{T}_0' + \tilde{Y}_{F0} - \tilde{T}_\infty\right)/\tilde{Y}_{O\infty}$ can be written in the dimensional form by $\left(c_p T_0' + Y_{F0} q_c - c_p T_\infty\right)/Y_{O\infty} q_c$, which can be approximated by $Y_{F0}/Y_{O\infty} \sim O(1)$ because q_c is much larger than either $c_p T_0'$ or $c_p T_\infty$. As we have proved in Appendix C, $|c_F| \sim O(1) \ll 1/Z_{st}$ and $|c_O| \sim O(1) \ll 1/Z_{st}$. Therefore, we can neglect the second term in the brace of Equation (28) and have

$$\chi_h = \frac{\alpha_D}{4Z_{st}} \tag{29}$$

To obtain the flame height in physical dimension, we should convert χ_h into its dimensional form. This is however mathematically cumbersome because, in the present piecewise power-law model, α_v in the vortex core is generally different from that of outside. For mathematical convenience, we can formally write the stream function for the power-law vortex in the form of

$$\psi = s(\xi)\eta^{\alpha_{v,\mathrm{eff}}} \tag{30}$$

where the effective exponent $\alpha_{v,\mathrm{eff}}$, will be determined shortly in the following subsection. Consequently, the parameter α_v in the coordinate transformation (18) shall be replaced by the effective exponent $\alpha_{v,\mathrm{eff}}$. According to Equations (10) and (18), we have

$$\chi_h = \frac{\alpha_{v,\mathrm{eff}}}{2}\frac{1}{\rho_0^2 u_0 r_0^2}\int_0^{x_h} \rho^2 D_F dx' = \frac{\alpha_{v,\mathrm{eff}}}{2}\frac{T_0^2}{u_0 r_0^2}\int_0^{x_h} \frac{D_F}{T^2} dx \tag{31}$$

where the isobaric approximation has been adopted because it is well justified in low Mach number flows [21]. Substituting Equation (31) to Equation (29), we have

$$\int_0^{x_h} T^{\alpha_T - 2} dx = \frac{Pe T_0^{\alpha_T - 2} d_0 \alpha_D}{8\alpha_{v,\mathrm{eff}} Z_{st}} \tag{32}$$

To derive Equation (32), we have considered the temperature-dependence of the mass diffusivity within the flame through the relation

$$D_F = D_{F0}\left(\frac{T}{T_0}\right)^{\alpha_T} \tag{33}$$

in which α_T is usually less than 2 [5, 28] and equal to 3/2 in the kinetic theory of gases employing the rigid-sphere model.

To facilitate an explicit and concise mathematical expression for the flame height, we denoted the following integral by T_m

$$T_m = \left[\frac{1}{x_h}\int_0^{x_h} T^{\alpha_T-2}dx\right]^{1/(\alpha_T-2)} \tag{34}$$

T_m can be treated as a representative temperature in the flame and exactly calculated by the following integration, after by substituting Equation (27) to (34):

$$T_m = \left[\frac{1}{x_h}\int_0^{x_h}\left[T_\infty + \frac{q_c Y_{O\infty}}{\sigma_{FO}c_p} + \left(T_0' - T_\infty - \frac{q_c Y_{O\infty}}{\sigma_{FO}c_p}\right) \times \int_0^\infty J_1(\omega)\exp\left(-\frac{\omega^2}{\alpha_D}\frac{1}{\rho_0^2 u_0 r_0^2}\int_0^x \rho^2 D_F dx'\right)d\omega\right]^{\alpha_T-2} dx\right]^{1/(\alpha_T-2)} \tag{35}$$

Substituting Eq. (34) into Eq. (32) we obtain the flame height of firewhirls as

$$\frac{x_h}{d_0} = \alpha_D \frac{2}{\alpha_{v,\text{eff}}}\left(\frac{T_m}{T_0}\right)^{2-\alpha_T}\frac{Pe}{16Z_{st}} \tag{36}$$

in which the effect of variable density and mass diffusivity are represented by the factor of $(T_m/T_0)^{2-\alpha_T}$, identical to that in our previous study [19]; the effect of strong vortex model is reflected in the factor $2/\alpha_{v,\text{eff}}$, which is formally the same as that obtained by Klimenko and William's [9], but the determination of $\alpha_{v,\text{eff}}$ is slightly different and will be discussed shortly in

following subsection; the newly identified effect of distinct mass diffusivities for fuel and oxidizer, represented by the factor α_D, will be discussed in detail in Section 4.

3.4 Determination of $\alpha_{v,\mathrm{eff}}$

To obtain an analytical form for the effective exponent $\alpha_{v,\mathrm{eff}}$ in Equation (36), we first recall that the flame height is determined by the farthermost axial location where both fuel and oxidizer vanish on the flame sheet. Because the axial location is sufficiently far away from the fuel pool, namely the flame height is substantially larger than the radius of the pool, the fuel and oxidizer profiles around the flame top can be described by their far-field solutions. Consequently, we can apply the alternative method, which was first proposed by Klimenko and Williams [9], to determine the flame height by making use of the far-field solutions of coupling functions (22) and (23). By equating the Eq. (22) to Eq. (23), we have

$$\xi_h = \frac{\alpha_D}{2AZ_{st}}\left[1 + Z_{st}\frac{(1-\alpha_D)}{\alpha_D}\frac{\left(\tilde{T}_0' + \tilde{Y}_{F0} - \tilde{T}_\infty\right)}{\tilde{Y}_{O\infty}}\right] \tag{37}$$

Using the same arguments on deriving Equation (29) from (33), Equation (37) can be simplified to

$$\xi_h = \frac{\alpha_D}{2AZ_{st}} \tag{38}$$

Rewriting Equation (38) in physical coordinates by using transformation (10), we have the alternative expression of the flame height based on the far-field solutions as

$$\frac{x_h}{d_0} = \alpha_D \frac{2}{A}\left(\frac{T_m}{T_0}\right)^{2-\alpha_T}\frac{Pe}{16Z_{st}} \tag{39}$$

Comparing Equation (39) with Equation (36), we can conclude that the effective exponent $\alpha_{v,\mathrm{eff}}$ should be the same as the integral factor A:

$$\alpha_{v,\text{eff}} = A = \frac{1}{\xi}\int_0^{\infty} \hat{u} \exp\left(\int_0^{\eta} \hat{v} d\eta\right) \eta d\eta$$

By substituting the axial and radial velocity profiles given by Equation (17b) in the above equation and assuming $s(\xi)$ as a linear function of ξ, we thus obtain an explicit expression for $\alpha_{v,\text{eff}}$ as

$$\alpha_{v,\text{eff}} = \alpha_v' - (\alpha_v' - \alpha_v) \exp\left(-\frac{\eta_c^{\alpha_v'}}{\alpha_v'}\right) \tag{40}$$

It is seen that $\alpha_{v,\text{eff}}$ relies on the radius of the vortex core as such it is equal to α_v in the limiting case of $\eta_c \to 0$ and to α_v' in the opposite limiting case of $\eta_c \to \infty$. Because there is lack of velocity measurement of firewhirl in Chuah *et al.*'s experiment, it is impossible for the present study to further determine the precise value of $\alpha_{v,\text{eff}}$ from Equation (40). As a result, $\alpha_{v,\text{eff}}$ will be treated as a fitting parameter within the range of 1.33 to 1.43, suggested by Klimenko and Williams[9]. It should be also noted that Equation (40) is a generalization to the result obtained by Klimenko and Williams [9] because the assumptions of constant density and mass diffusivity are removed in the present study and because the inner regime is not restricted to the Burgers vortex.

4. "Enhancement" and "Reduction" Mechanisms of Flame Height

The expression for the flame height features a linear relation between the diameter-scaled flame height, x_h/d_0 and the modified Peclet number, $Pe/(16Z_{st})$; the gradient of the linearity is affected by the three multiplicative factors, namely, $(T_m/T_0)^{2-\alpha_T}$, $2/\alpha_{v,\text{eff}}$ and α_D. The physical significance of each factor will be discussed in detail as follows.

The factor $(T_m/T_0)^{2-\alpha_T}$ characterizes the effect of variable density and mass diffusivity on the flame height, and has been identified and thoroughly discussed in the recent study of Yu and Zhang [19]. In summary, $(T_m/T_0)^{2-\alpha_T}$ provides an "enhancement" mechanism to the flame height because it is always larger than unity. Specifically, the representative temperature T_m, defined by Equation (34), is always larger than T_0, and the exponent α_T of a power-law function characterizing the temperature dependence of mass diffusivity is always smaller than 2 (for example, $\alpha_T = 1.5$ according to the kinetic theory employing the rigid sphere model and $\alpha_T = 1.8$ as

suggested by Chuah *et al*. [5]). The enhancement mechanism of the variable density and mass diffusivity can be physically interpreted by that the flow density decreases with increasing the flow temperature, that the flow with reduced density becomes more readily to be advected to larger height, leading to that the flame height tends to increase. For illustration, Figure 2 shows the ethanol flame contours, as an example, in the stream function coordinates (χ,ζ), the density-mass diffusivity-weighted coordinates (ξ,η), and the physical coordinates (x,r). The flame contour calculated by ignoring the density variation is also shown for comparison. It is seen that the variable density tends to expand the flame contour in both radial and axial directions without significantly changing their shape, leading to an increase of flame height [19].

The factor $2/\alpha_{v,\mathrm{eff}}$, which is formally identical to the correction factor identified by Klimenko and Williams [9], characterizes another "enhancement" mechanism for the flame height because the power-law strong vortex ($\alpha_{v,\mathrm{eff}} < 2$) generates more rapid axial flow near the axis, leading to more intensive axial stretching than the Burgers vortex ($\alpha_{v,\mathrm{eff}} = 2$). In consequence, the flame top is risen to a larger height by a factor of $2/\alpha_{v,\mathrm{eff}}$. It should be noted that the parameter $\alpha_{v,\mathrm{eff}}$ differs from either α_v' in the vortex core or α_v in the outer regime. It is physically improper to adopt a constant exponent $\alpha_v \neq 2$ for the entire flow field without either causing a singularity of axial velocity at the axis or violating the boundary condition at the radial infinity. The mathematical representative of the combining effects of both exponents is the effective exponent $\alpha_{v,\mathrm{eff}}$, whose analytical expression is given by Equation (40). Following Klimenko and Williams' approach [9], $\alpha_{v,\mathrm{eff}}$ will be treated as a fitting parameter in the present study because its precise determination is impossible due to the insufficient experimental observations on the vortical flow field in firewhirls. To facilitate the comparison with Klimenko and Williams' study, we shall use $\alpha_{v,\mathrm{eff}} = 1.33$ and $\alpha_{v,\mathrm{eff}} = 1.43$ recommended in their study [9].

The factor α_D characterizes the effect of distinct mass diffusivities of fuel and oxidizer, which can lead to a substantial reduction of the flame height, as will be shown shortly. The underlying physics is that the mass diffusivities of common liquid hydrocarbons are smaller than that of oxygen in air, because the binary mass diffusivity decreases with increasing the molecular weight of the concerned species according to the Chapman-Enskog theory [22]. The ratio of fuel mass diffusivity to oxidizer mass diffusivity depends on the fuel type and we have $\alpha_D = 0.85$ for methanol,

$\alpha_D = 0.70$ for ethanol, and $\alpha_D = 0.52$ for 2-propanol [22]. Consequently, the required higher gradient of fuel mass fraction within the firewhirl flame causes the flame contour to move inside to the fuel side and therefore lead to the reduction of flame height.

Equation (36) is the expression for the flame heights of firewhirls, which can degenerate to that of Chuah *et al.* [5] in the case of $\alpha_{v,\text{eff}} = 2$, $\alpha_T = 2$ and $\alpha_D = 1$, to that of Klimenko and Williams [9] in the case of $\alpha_T = 2$ and $\alpha_D = 1$, and to that of Yu and Zhang [19] in the case of $\alpha_{v,\text{eff}} = 2$ and $\alpha_D = 1$.

To illustrate the comparison between different theories with experimental results, Figure 3 shows the theoretical predictions by Equation (36) with different combinations of $\alpha_{v,\text{eff}}$ and α_T. In each subplot for a combination of $\alpha_{v,\text{eff}}$ and α_T, the mass diffusivity ratio α_D varies according to the fuel types adopted in Chuah *et al.*'s study [5].

First, we discuss about the situation of $\alpha_D = 1$, which is represented by the dashed line in each subplot. It is seen that x_h/d_0 tends to increase with decreasing either $\alpha_{v,\text{eff}}$ or α_T or both. Within the physically realistic ranges of $\alpha_{v,\text{eff}}$ and α_T, namely, $1.33 \leq \alpha_{v,\text{eff}} \leq 1.43$ and $1.5 \leq \alpha_T \leq 1.8$, the theoretical predictions always overshoot the experimental data. This means that the combined "enhancement" mechanisms due to the strong power-law vortex and variable physical properties produce a considerable overestimation to the flame height, which must be counteracted by some "reduction" mechanism.

The "reduction" mechanism owing to $\alpha_D < 1$ generates anew good theoretical predictions of flame height, presented as the solid lines in each subfigure of Figure 3, with the experimental data. The degree of the "reduction" depends on the fuel types so that it is more substantial for burning 2-propanol than for burning methanol. The discrepancy may be attributed to that the flame temperature of propanol firewhirl is higher than that of the other two alcohols and using a higher propanol flame temperature can improve the theoretical predictions, as already pointed out by Yu and Zhang [19]. In the present calculations, the flame temperature for all liquid fuels is set as 1300K as suggested by Chua *et al.* [5] and further analysis of the propanol firewhirls is impossible without more details and uncertainty quantification about the experiments.

5. Concluding Remarks

A theory of the flame height of firewhirls has been established in the present study by means of coupling function formulation, with a particular interest in approximately combining variable physical properties, a power-law vortex model and a mass-diffusivity-ratio model in the theory. Although the specified boundary conditions and the adopted approximations remain to be further verified, interesting and useful understanding on the problem has been obtained.

In terms of the approximate matching solutions of the coupling functions, the theory yields a composite expression for the flame height, which can degenerate to those obtained in the previous studies [5, 9, 19], in the expression, the linearity between the diameter-scaled flame height x_h/d_0 and modified Peclet number $Pe/(16Z_{st})$ remains; the slope of the linear reaction is characterized by three factors, each of which interprets independent and indispensable physics. Specifically, the effect of variable density and diffusivities, characterized by $\left(T_m/T_0\right)^{2-\alpha_T}$, results in reduced flow inertia and thus tends to increase the flame height. The effect of the power-law strong vortex, characterized by $2/\alpha_{v,\mathrm{eff}}$ with $\alpha_{v,\mathrm{eff}} < 2$, leads to the intensified axial stretching of the vortical flow near the axis thus causes the flame tip at the axis to grow higher. The effect of the distinct mass diffusivities of fuel and oxidizer, characterized by $\alpha_D < 1$, requires a larger gradient of fuel mass fraction within the flame contour, moves the flame closer to the fuel pool, and thus reduces the flame height. Combining the first two effects yields a considerable overestimation for the flame height, which can be satisfactorily corrected by the third factor, resulting good agreement with the experimental results.

Similar to all the previous theoretical studies, the present study formulates and analyzes the circulation-controlled firewhirls in an open space (semi-infinite space) instead of enclosed by side walls in the experiments [5]. For confined firewhirls, the wall-to-pan ratio is an important experimental factor, especially if it is insufficiently large. Physically, a small wall-to-pan size ratio results in more heat loss from the flame, which in turn affects the flame temperature and the flame height, requiring the consideration of finite-rate flame chemistry and heat loss mechanism in future studies. In addition, the wall effect in producing vortices of various strength should be taken into account and the applicability of the idealized power-law or Burgers vortex models needs to be reexamined. Future studies are also merited for considering the effects of non-unity Lewis number. Implementing $Le \neq 1$ is analytically infeasible for the existing theoretical approaches based on

either mixture fraction or coupling function. Numerical simulation with modelling differential diffusions of species may play an important role in studying the non-unity Lewis number effects.

Acknowledgement

This work was supported by the Hong Kong RGC/GRF (operating under contract numbers PolyU 152217/14E and 152651/16E) and partly by the Hong Kong Polytechnic University (G-UA2M and G-YBGA).

Appendix A

The nondimensional governing equation for the coupling function β_F in physical coordinates can be expressed as

$$\tilde{\rho}\tilde{u}\frac{\partial \beta_F}{\partial \tilde{x}} + \tilde{\rho}\tilde{v}\frac{\partial \beta_F}{\partial \tilde{r}} = \frac{1}{Pe}\frac{\partial}{\partial \tilde{x}}\left(\tilde{\rho}\widetilde{D}_F\frac{\partial \beta_F}{\partial \tilde{x}}\right) + \frac{1}{Pe}\frac{1}{\tilde{r}}\frac{\partial}{\partial \tilde{r}}\left(\tilde{\rho}\widetilde{D}_F\tilde{r}\frac{\partial \beta_F}{\partial \tilde{r}}\right) \tag{A1}$$

We applied a density-mass-diffusivity-weighted coordinate transformation (10) to Equation (A1) and obtained the following spatial derivatives

$$\tilde{\rho}\tilde{u}\frac{\partial}{\partial \tilde{x}} = \frac{1}{Pe}\tilde{\rho}^3\widetilde{D}_F\tilde{u}\left[2\frac{\partial}{\partial \xi} + 2h\frac{\partial}{\partial \eta}\right] \tag{A2}$$

$$\tilde{\rho}\tilde{v}\frac{\partial}{\partial \tilde{r}} = \frac{1}{Pe}\tilde{\rho}^3\widetilde{D}_F\tilde{v}\left[2g\frac{\partial}{\partial \xi} + \frac{Pe}{\tilde{\rho}\widetilde{D}_F}\frac{\partial}{\partial \eta}\right] \tag{A3}$$

$$\begin{aligned}\frac{1}{Pe}\frac{\partial}{\partial \tilde{x}}\left(\tilde{\rho}\widetilde{D}_F\frac{\partial}{\partial \tilde{x}}\right) &= \frac{\tilde{\rho}^3\widetilde{D}_F}{Pe}\frac{4}{Pe^2\tilde{\rho}}\left[\frac{\partial}{\partial \xi}\left(\tilde{\rho}^3\widetilde{D}_F^2\frac{\partial}{\partial \xi}\right) + \frac{\partial}{\partial \xi}\left(\tilde{\rho}^3\widetilde{D}_F^2h\frac{\partial}{\partial \eta}\right) + h\frac{\partial}{\partial \eta}\left(\tilde{\rho}^3\widetilde{D}_F^2\frac{\partial}{\partial \xi}\right)\right.\\ &\left. + h\frac{\partial}{\partial \eta}\left(\tilde{\rho}^3\widetilde{D}_F^2h\frac{\partial}{\partial \eta}\right)\right]\end{aligned}$$

(A4)

$$\frac{1}{Pe}\frac{1}{\tilde{r}}\frac{\partial}{\partial\tilde{r}}\left(\tilde{\rho}\widetilde{D}_F\tilde{r}\frac{\partial}{\partial\tilde{r}}\right) = \frac{\tilde{\rho}^3\widetilde{D}_F}{Pe}\left[\frac{4g}{Pe^2\tilde{\rho}\tilde{r}}\frac{\partial}{\partial\xi}\left(\tilde{\rho}^3\widetilde{D}_F^2\tilde{r}g\frac{\partial}{\partial\xi}\right)+\frac{2g}{Pe\tilde{\rho}\tilde{r}}\frac{\partial}{\partial\xi}\left(\tilde{\rho}^2\widetilde{D}_F\tilde{r}\frac{\partial}{\partial\eta}\right)+\frac{2}{Pe\tilde{\rho}^2\widetilde{D}_F\tilde{r}}\frac{\partial}{\partial\eta}\left(\tilde{\rho}^3\widetilde{D}_F^2\tilde{r}g\frac{\partial}{\partial\xi}\right)+\frac{1}{\tilde{\rho}^2\widetilde{D}_F\tilde{r}}\frac{\partial}{\partial\eta}\left(\tilde{\rho}^2\widetilde{D}_F\tilde{r}\frac{\partial}{\partial\eta}\right)\right]$$

(A5)

where $h(\tilde{x},\tilde{r})=\frac{Pe}{2\tilde{\rho}^2\widetilde{D}_F}\int_0^{\tilde{r}}\frac{\partial\tilde{\rho}}{\partial\tilde{x}}dr'$ and $g(\tilde{x},\tilde{r})=\frac{1}{\tilde{\rho}^2\widetilde{D}_F}\int_0^{\tilde{x}}\frac{\partial}{\partial\tilde{r}}\left(\tilde{\rho}^2\widetilde{D}_F\right)dx'$.

Substituting Equations (A2)-(A5) into Equation (A1), cancelling out the common term $\tilde{\rho}^3\widetilde{D}_F/Pe$, and denoting $\hat{u}=2\tilde{u}+2g\tilde{v}$ and $\hat{v}=2h\tilde{u}+Pe\tilde{v}/\left(\tilde{\rho}\widetilde{D}_F\right)$, we have Equation (11):

$$\hat{u}\frac{\partial\beta_F}{\partial\xi}+\hat{v}\frac{\partial\beta_F}{\partial\eta}=\frac{4}{Pe^2}\frac{1}{\tilde{\rho}}\left(\frac{\partial}{\partial\xi}+h\frac{\partial}{\partial\eta}\right)\left[\tilde{\rho}^3\widetilde{D}_F^2\left(\frac{\partial\beta_F}{\partial\xi}+h\frac{\partial\beta_F}{\partial\eta}\right)\right]+\left(\frac{2}{Pe}\frac{g}{\tilde{\rho}\tilde{r}}\frac{\partial}{\partial\xi}+\frac{1}{\tilde{\rho}^2\widetilde{D}_F\tilde{r}}\frac{\partial}{\partial\eta}\right)\left(\frac{2\tilde{\rho}^3\widetilde{D}_F^2g\tilde{r}}{Pe}\frac{\partial\beta_F}{\partial\xi}+\tilde{\rho}^2\widetilde{D}_F\tilde{r}\frac{\partial\beta_F}{\partial\eta}\right)$$

The derivation of the transport equation for the coupling function β_O is almost the same, except all the diffusion terms on the RHS must be divided by the constant α_D, giving Equation (12).

Appendix B

According to Equation (13) the velocity components in physical coordinates can be transformed to $\tilde{u}$ and $\tilde{v}$ in the $\xi-\eta$ coordinates:

$$\tilde{u}=\frac{\hat{u}Pe/\left(2\tilde{\rho}\widetilde{D}_F\right)-g\hat{v}}{Pe/\left(2\tilde{\rho}\widetilde{D}_F\right)-gh}$$

(B1)

$$\tilde{v}=-\frac{\hat{u}h(\tilde{x},\tilde{r})-\hat{v}}{Pe/\left(2\tilde{\rho}\widetilde{D}_F\right)-gh}$$

(B2)

In the power law vortex model, $\hat{u}$ and $\hat{v}$ are expressed by Equation (17b) generated from the piecewise stream function (17a). Substituting Equation (17b) into Equations (B1) and (B2), we obtain the velocity components in physical coordinates:

$$\tilde{u} = \left[\frac{\alpha_v' Pe}{2\tilde{\rho}\widetilde{D}_F} s\left(\frac{2}{Pe}\int_0^{\tilde{x}} \tilde{\rho}^2 \widetilde{D}_F dx'\right)\left(\int_0^{\tilde{r}} \tilde{\rho} dr'\right)^{\alpha_v'-2} + g\frac{ds}{d\tilde{x}}\left(\frac{2}{Pe}\int_0^{\tilde{x}} \tilde{\rho}^2 \widetilde{D}_F dx'\right)\left(\int_0^{\tilde{r}} \tilde{\rho} dr'\right)^{\alpha_v'-1}\right]\left[\frac{Pe}{2\tilde{\rho}\widetilde{D}_F} - gh\right]^{-1}, \quad \tilde{r} < \tilde{r}_c \tag{B3}$$

$$\tilde{u} = \left(\int_0^{\tilde{r}_c} \tilde{\rho} dr'\right)^{\alpha_v'-\alpha_v}\left[\frac{\alpha_v Pe}{2\tilde{\rho}\widetilde{D}_F} s\left(\frac{2}{Pe}\int_0^{\tilde{x}} \tilde{\rho}^2 \widetilde{D}_F dx'\right)\left(\int_0^{\tilde{r}} \tilde{\rho} dr'\right)^{\alpha_v-2} + g\frac{ds}{d\tilde{x}}\left(\frac{2}{Pe}\int_0^{\tilde{x}} \tilde{\rho}^2 \widetilde{D}_F dx'\right)\left(\int_0^{\tilde{r}} \tilde{\rho} dr'\right)^{\alpha_v-1}\right]\left[\frac{Pe}{2\tilde{\rho}\widetilde{D}_F} - gh\right]^{-1}, \quad \tilde{r} \geq \tilde{r}_c \tag{B4}$$

$$\tilde{v} = \left[\alpha_v' hs\left(\frac{2}{Pe}\int_0^{\tilde{x}} \tilde{\rho}^2 \widetilde{D}_F dx'\right)\left(\int_0^{\tilde{r}} \tilde{\rho} dr'\right)^{\alpha_v'-2} + \frac{ds}{d\tilde{x}}\left(\frac{2}{Pe}\int_0^{\tilde{x}} \tilde{\rho}^2 \widetilde{D}_F dx'\right)\left(\int_0^{\tilde{r}} \tilde{\rho} dr'\right)^{\alpha_v'-1}\right]\left[hg - \frac{Pe}{2\tilde{\rho}\widetilde{D}_F}\right]^{-1}, \quad \tilde{r} < \tilde{r}_c \tag{B5}$$

$$\tilde{v} = \left(\int_0^{\tilde{r}_c} \tilde{\rho} dr'\right)^{\alpha_v'-\alpha_v}\left[\alpha_v hs\left(\frac{2}{Pe}\int_0^{\tilde{x}} \tilde{\rho}^2 \widetilde{D}_F dx'\right)\left(\int_0^{\tilde{r}} \tilde{\rho} dr'\right)^{\alpha_v-2} + \frac{ds}{d\tilde{x}}\left(\frac{2}{Pe}\int_0^{\tilde{x}} \tilde{\rho}^2 \widetilde{D}_F dx'\right)\left(\int_0^{\tilde{r}} \tilde{\rho} dr'\right)^{\alpha_v-1}\right]\left[hg - \frac{Pe}{2\tilde{\rho}\widetilde{D}_F}\right]^{-1}, \quad \tilde{r} \geq \tilde{r}_c \tag{B6}$$

It is extremely complex to directly check the consistence of (B3)-(B6) with the continuity equation. We can however readily check it for degenerate situations. Under the situation of constant density and mass diffusivity and for $\alpha_v = \alpha_v' = 2$, the velocity components (B3) to (B6) can be written by

$$\tilde{u} = 2s\left(\frac{2\tilde{\rho}^2\widetilde{D}_F\tilde{x}}{Pe}\right) \tag{B7}$$

$$\tilde{v} = -\frac{2\tilde{\rho}^2\widetilde{D}_F}{Pe}\frac{d}{d\tilde{x}}\left[s\left(\frac{2\tilde{\rho}^2\widetilde{D}_F\tilde{x}}{Pe}\right)\right]\tilde{r} \tag{B8}$$

which accords with the Burgers vortex with constant physical properties except that the axial coordinate is stretched by a factor of $2\tilde{\rho}^2\widetilde{D}_F/Pe$ according to the coordinate transformation (10). Substituting Equations (B7) and (B8) into the continuity equation with constant density

$$\frac{\partial(\tilde{u}\tilde{r})}{\partial\tilde{x}} + \frac{\partial(\tilde{v}\tilde{r})}{\partial\tilde{r}} = 0 \tag{B9}$$

we can find that the equation holds exactly.

Under the situation of constant density and mass diffusivity but for $\alpha_v' = 2$, the flow velocities inside the vortex core are identical to Equations (B7) and (B8), and those outside the vortex core are given by

$$\tilde{u} = \alpha_v s\left(\frac{2\tilde{\rho}^2\widetilde{D}_F\tilde{x}}{Pe}\right)\left(\frac{1}{\tilde{r}_c}\right)^{\alpha_v-2}\tilde{r}^{\alpha_v-2}, \qquad \tilde{r} \geq \tilde{r}_c \tag{B10}$$

$$\tilde{v} = -\frac{2\tilde{\rho}^2\widetilde{D}_F}{Pe}\left(\frac{1}{\tilde{r}_c}\right)^{\alpha_v-2}\frac{d}{d\tilde{x}}\left[s\left(\frac{2\tilde{\rho}^2\widetilde{D}_F\tilde{x}}{Pe}\right)\right]\tilde{r}^{\alpha_v-1}, \qquad \tilde{r} \geq \tilde{r}_c \tag{B11}$$

(B10) and (B11), together with (B7) and (B8), can be regarded as a generalized, nondimensional form of the strong vortex with constant density, which was formulated by Klimenko [9, 20]. The consistency of these velocity components with Equation (B9) can be readily verified.

Under the situation of slow variation of $\tilde{\rho}^2\widetilde{D}_F$ in radial direction, i.e., $\int_0^{\tilde{x}}\frac{\partial}{\partial\tilde{r}}\left(\tilde{\rho}^2\widetilde{D}_F\right)dx' \approx 0$, and slow variation of $\tilde{\rho}$ in axial direction, i.e., $\int_0^{\tilde{r}}\frac{\partial\tilde{\rho}}{\partial\tilde{x}}dr' \approx 0$, and for $\alpha_v = \alpha_v' = 2$, we have

$$\tilde{u} = 2s\left(\frac{2}{Pe}\int_0^{\tilde{x}}\tilde{\rho}^2\widetilde{D}_F dx'\right)$$

(B12)

$$\tilde{v} = -\frac{2\tilde{\rho}\widetilde{D}_F}{Pe}\left[\frac{d}{d\tilde{x}}s\left(\frac{2}{Pe}\int_0^{\tilde{x}}\tilde{\rho}^2\widetilde{D}_F dx'\right)\left(\int_0^{\tilde{r}}\tilde{\rho}dr'\right)\right]$$

(B13)

which can be regarded as the generalization of the variable-density Burgers vortex model proposed by Yu and Zhang [19] without assuming that the $s(\xi)$ is a linear function of ξ. Because of the variable physical property effects included in Equations (B12) and (B13) in the forms of integration, we have to invoke the additional assumption of constant Chapman-Rubesin-like parameter to satisfy the continuity equation with variable density.

$$\frac{\partial(\tilde{\rho}\tilde{u}\tilde{r})}{\partial\tilde{x}} + \frac{\partial(\tilde{\rho}\tilde{v}\tilde{r})}{\partial\tilde{r}} = 0$$

(B14)

Appendix C

To estimate the value of c_F and c_O at the flame height location, we note that they must have the same order of magnitude due to their similar role in the matching solutions. Thus, we can approximately regard them as $c_F \sim c_O \sim c$, which is evaluated explicitly at the flame height location by replacing c_F and c_O by c in Eq. (28), yielding

$$c = \frac{4\chi_h\tilde{Y}_{O\infty} + \alpha_D\left(\tilde{T}_0' - \tilde{T}_\infty - \tilde{Y}_{O\infty}\right) - \left(\tilde{Y}_{F0} + \tilde{T}_0' - \tilde{T}_\infty\right)}{(\alpha_D - 1)\left(2\tilde{T}_0' - 2\tilde{T}_\infty - \tilde{Y}_{O\infty} + \tilde{Y}_{F0}\right)}$$

(C1)

Since the values of $\tilde{T}_0'$ and $\tilde{T}_\infty$, i.e., the temperatures being scaled by q_c/c_p, are much smaller than $\tilde{Y}_{F0}$ and $\tilde{Y}_{O\infty}$, the quantity c can be very well approximated by

$$c \approx \frac{1 - 4\chi_h Z_{st} - (1-\alpha_D)Z_{st}}{(1-\alpha_D)(1-2Z_{st})}$$

(C2)

Recalling that the stoichiometric mixture fraction Z_{st} is a small quantity, α_D is of order of unity, and the combination $4\chi_h Z_{st}$ is of order of unity as well, the quantity c should also be of order unity, i.e.,

$$c \sim O(1)$$

Reference

[1] F. Battaglia, K.B. McGrattan, R.G. Rehm, H.R. Baum, Simulating fire whirls, Combustion Theory and Modelling 4 (2000) 123-138.

[2] F. Battaglia, R.G. Rehm, H.R. Baum, The fluid mechanics of fire whirls: An inviscid model, Physics of Fluids 12 (2000) 2859-2867.

[3] K.H. Chuah, G. Kushida, The prediction of flame heights and flame shapes of small fire whirls, Proceedings of the Combustion Institute 31 (2007) 2599-2606.

[4] K.H. Chuah, K. Kuwana, K. Saito, Modeling a fire whirl generated over a 5-cm-diameter methanol pool fire, Combustion and Flame 156 (2009) 1828-1833.

[5] K.H. Chuah, K. Kuwana, K. Saito, F.A. Williams, Inclined fire whirls, Proceedings of the Combustion Institute 33 (2011) 2417-2424.

[6] H.W. Emmons, S.-J. Ying. The fire whirl. Symposium (International) on Combustion; 1967: Elsevier. p. 475-488.

[7] Y. Hayashi, K. Kuwana, T. Mogi, R. Dobashi, Influence of Vortex Parameters on the Flame Height of a Weak Fire Whirl via Heat Feedback Mechanism, Journal of Chemical Engineering of Japan 46 (2013) 689-694.

[8] L.H. Hu, J.J. Hu, S. Liu, W. Tang, X.Z. Zhang, Evolution of heat feedback in medium pool fires with cross air flow and scaling of mass burning flux by a stagnant layer theory solution, Proceedings of the Combustion Institute 35 (2015) 2511-2518.

[9] A.Y. Klimenko, F.A. Williams, On the flame length in firewhirls with strong vorticity, Combustion and Flame 160 (2013) 335-339.

[10] K. Kuwana, S. Morishita, R. Dobashi, K.H. Chuah, K. Saito, The burning rate's effect on the flame length of weak fire whirls, Proceedings of the Combustion Institute 33 (2011) 2425-2432.

[11] K. Kuwana, K. Sekimoto, T. Minami, T. Tashiro, K. Saito, Scale-model experiments of moving fire whirl over a line fire, Proceedings of the Combustion Institute 34 (2013) 2625-2631.

[12] K. Kuwana, K. Sekimoto, K. Saito, F.A. Williams, Scaling fire whirls, Fire Safety Journal 43 (2008) 252-257.

[13] J. Lei, N. Liu, K. Satoh, Buoyant pool fires under imposed circulations before the formation of fire whirls, Proceedings of the Combustion Institute 35 (2015) 2503-2510.

[14] J. Lei, N.A. Liu, L.H. Zhang, K. Satoh, Temperature, velocity and air entrainment of fire whirl plume: A comprehensive experimental investigation, Combustion and Flame 162 (2015) 745-758.

[15] J.A. Lei, N.A. Liu, L.H. Zhang, H.X. Chen, L.F. Shu, P. Chen, Z.H. Deng, J.P. Zhu, K. Satoh, J.L. de Ris, Experimental research on combustion dynamics of medium-scale fire whirl, Proceedings of the Combustion Institute 33 (2011) 2407-2415.

[16] K. Zhou, N. Liu, K. Satoh, Experimental research on burning rate, vertical velocity and radiation of medium-scale fire whirls, Fire Safety Science 10 (2011) 681-691.
[17] K. Zhou, N. Liu, L. Zhang, K. Satoh, Thermal radiation from fire whirls: revised solid flame model, Fire Technology 50 (2014) 1573-1587.
[18] R. Zhou, Z.N. Wu, Fire whirls due to surrounding flame sources and the influence of the rotation speed on the flame height, Journal of Fluid Mechanics 583 (2007) 313-345.
[19] D. Yu, P. Zhang, On the flame height of circulation-controlled firewhirls with variable density, Proceedings of the Combustion Institute 36 (2017) 3097–3104.
[20] A.Y. Klimenko, Strong swirl approximation and intensive vortices in the atmosphere, Journal of Fluid Mechanics 738 (2014) 268-298.
[21] C.K. Law, Combustion physics, Cambridge University Press, 2006.
[22] E.L. Cussler, Diffusion: mass transfer in fluid systems, Cambridge University Press, 2009.
[23] K.K. Kuo, Principles of Combustion, John Wiley & Sons, Inc, 2005.
[24] F. Williams, Combustion Theory The Benjamin/Cummings, 1985.
[25] F.W. Matting, General solution of the laminar compressible boundary layer in the stagnation region of blunt bodies in axisymmetric flow, (1964).
[26] P.M. Chung, Chemically reacting nonequilibrium boundary layers, Advances in heat transfer 2 (1965) 109-270.
[27] N. Peters, Turbulent combustion, Cambridge University Press, 2000.
[28] R.A. Yetter, I. Glassman, H.C. Gabler, Asymmetric whirl combustion: a new low NOx approach, Proceedings of the combustion institute 28 (2000) 1265-1272.

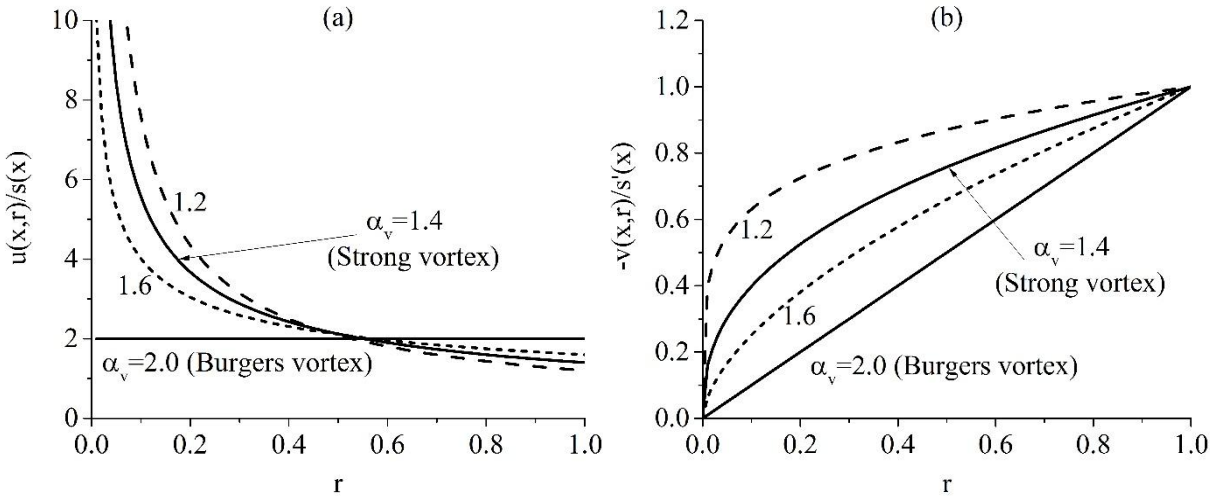

Figure 1. The radial profiles of (a) the axial velocity component and (b) the radial velocity component of power-law vortices.

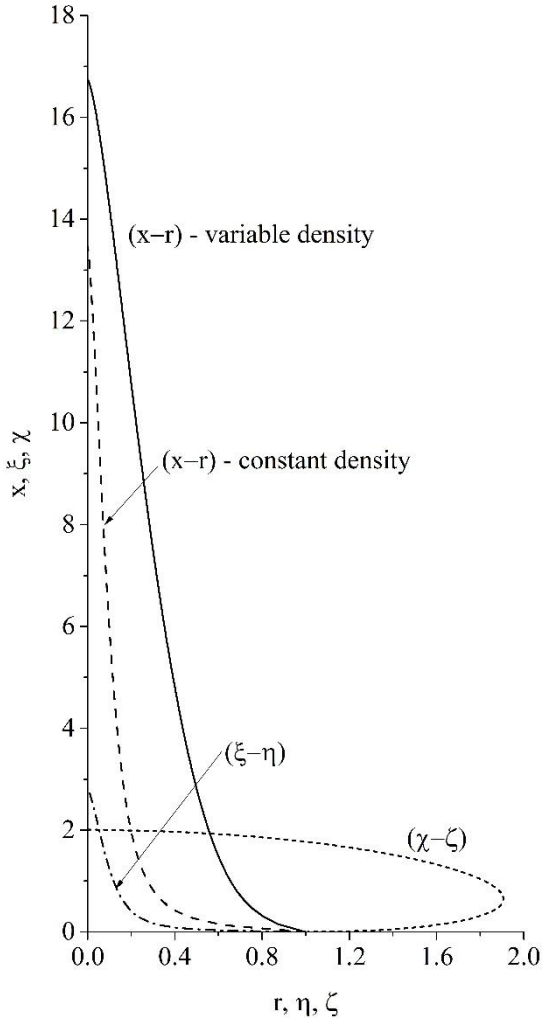

Figure 2. Ethanol firewhirl contours in various coordinates.

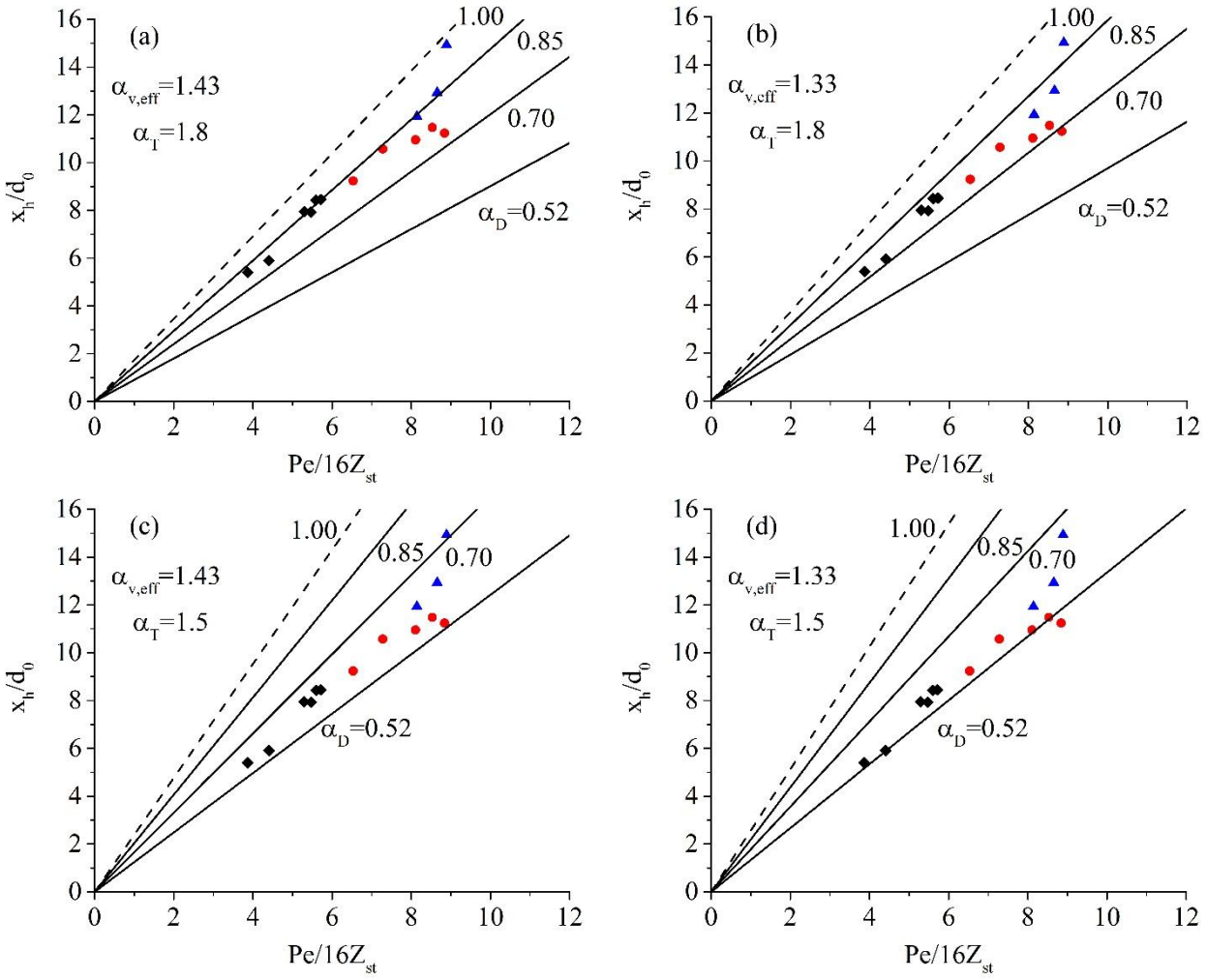

Figure 3. Diameter-scaled flame height plotted against modified Peclet number. Solid symbols represent experimental data from Chuah *et al.* [5] for various alcohols: methanol (♦), ethanol (●) and 2-propanol (▲). The lines represent the theoretical predictions with various ratios of mass diffusivities of fuel and oxidizer.